

# Theoretical study of the gas-phase elimination kinetics of several heterocyclic carbamates

Mariana Graterol,<sup>1</sup> Tania Cordova<sup>1</sup> and G. Chuchani<sup>2\*</sup>

<sup>1</sup>Laboratorio de Físico-Química Orgánica. Escuela de Química, Facultad de Ciencias, Universidad Central de Venezuela, Apartado 1020-A, Caracas, Venezuela

<sup>2</sup>Centro de Química, Instituto Venezolano de Investigaciones Científicas (IVIC), Apartado 21827, Caracas 1020-A, Venezuela

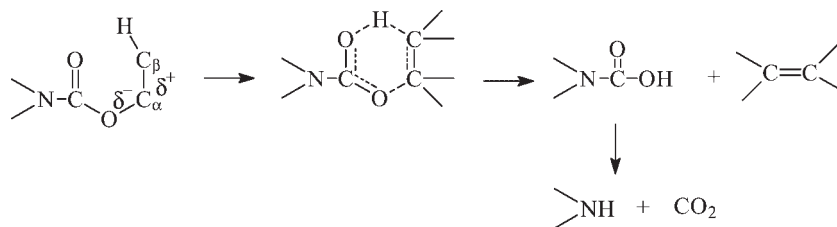
Received 7 November 2005; revised 12 December 2005; accepted 6 January 2006

**ABSTRACT:** The homogeneous, unimolecular, gas-phase elimination kinetics of several heterocyclic carbamates was studied at the MP2/6-31G level of theory under the average experimental conditions for each substrate. The elimination products for these carbamates are the corresponding carbamic acid and isobutylene. The intermediate acids are unstable and decarboxylate at the reaction temperature. Calculated thermodynamic and kinetic parameters are in good agreement with the experimental values, displaying the same reactivity order observed experimentally. An increase in the electron-withdrawing effect of the substituent on the carbamate nitrogen, increases the elimination rate. Transition state structures are described as six-membered rings with some departure from planarity. NBO charge analysis reveals strong polarization at the O(ester)  $\delta^-$ —C $\delta^+$  bond. Bond indexes and synchronicity parameters are consistent with a concerted polar type of mechanism with O(ester)  $\delta^-$ —C $\delta^+$  bond breaking as the most important process. Copyright © 2007 John Wiley & Sons, Ltd.

**KEYWORDS:** kinetics; unimolecular elimination; pyrolysis; heterocyclic carbamates; semi-empirical, 'ab initio' calculations; reaction mechanism; transition state structure

## INTRODUCTION

The elimination rates for 2-alkylethyl *N,N*-diethylcarbamates<sup>1</sup> were found to be consistent with the sequence of the equivalent rate for the corresponding 2-alkylethyl *N,N*-dimethylcarbamates.<sup>2</sup> That is, the elimination of the olefin is in the order *tert*-butyl > isopropyl > ethyl. The mechanism of these reactions (1) is thought to proceed through a concerted six-membered cyclic transition state (TS) structure, where the C $\alpha$ —O bond polarization, in the direction of C $\alpha^{\delta+}$ —O $\delta^-$ , is the rate determining step.



The (CH<sub>3</sub>CH<sub>2</sub>)<sub>2</sub>N substituent at the acid side of these esters was found to slightly decrease the rate compared to the (CH<sub>3</sub>)<sub>2</sub>N substituent. The small difference has been attributed to the greater electron release of the CH<sub>3</sub>CH<sub>2</sub> to the N atom than the CH<sub>3</sub>. On replacing the methyl group

of (CH<sub>3</sub>)<sub>2</sub>NCOOCH<sub>2</sub>CH<sub>3</sub> with one or two phenyl groups,<sup>3</sup> a significant decrease in the rate has been observed. This suggests that steric factors affect the process of ethylene elimination.

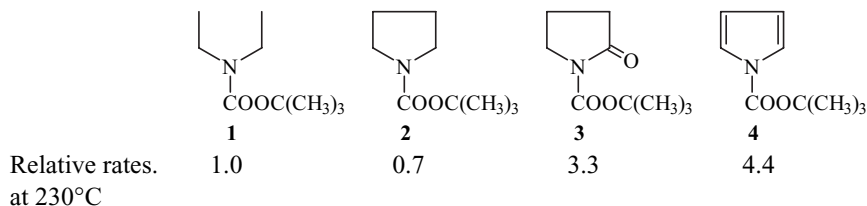
Recently, a Møller–Plesset MP2/6–31G method used to study the gas-phase elimination of 2-substituted alkyl ethyl methylcarbamates<sup>4</sup> was found to support the concerted non-synchronous six-membered cyclic TS type of mechanism [reaction (1)].

In a study on heterocyclic carbamates,<sup>5</sup> the saturated heterocyclic carbamates showed a decrease in elimination

rates due to electronic factors. However, heterocyclic carbamates with the N atom delocalizing its electrons with  $\Pi$ -bonds present in the ring showed enhanced rates due to resonance interactions (scheme 1).

This study examines the potential energy surface (PES) at the MP2/6-31G level of theory in order to determine the kinetic and thermodynamic parameters for the elucidation of the nature of the gas-phase molecular elimination of the heterocyclic carbamates depicted in scheme 1.

\*Correspondence to: G. Chuchani, Centro de Química, Instituto Venezolano de Investigaciones Científicas (IVIC), Apartado 21827, Caracas 1020-A, Venezuela.  
E-mail: chuchani@iviv.ve



Scheme 1

## COMPUTATIONAL METHODS AND MODELS

Electronic structure calculations using the Møller–Plesset perturbation method MP2 with a 6-31G basis set as implemented in Gaussian 98W<sup>6</sup> were performed to study the kinetics and mechanisms of the gas-phase elimination reactions of *t*-butyl carbamates with different substituents on the nitrogen. The Berny analytical gradient optimization routines were used. The requested convergence on the density matrix was  $10^{-9}$  atomic units, the threshold value for maximum displacement was 0.0018 Å, and that for the maximum force was 0.00045 Hartree/Bohr. The nature of the stationary points was established by calculating and diagonalizing the Hessian matrix (force constant matrix). TS structures were characterized by means of normal-mode analysis. The transition vector (TV) associated with the unique imaginary frequency, that is, the eigenvector associated with the unique negative eigenvalue of the force constant matrix, was characterized.

Frequency calculations were carried out to obtain thermodynamic quantities such as the zero point vibrational energy (ZPVE), temperature corrections  $E(T)$  and absolute entropies  $S(T)$ . Temperature corrections and absolute entropies were obtained, assuming ideal gas behavior, from the harmonic frequencies and moments of inertia using standard methods<sup>7</sup> at the average temperature and pressure values for the experimental range. Scaling factors for frequencies and zero point energies for the MP2 methods used are taken from the literature.<sup>8</sup>

The first order rate coefficient  $k(T)$  was calculated using the TST<sup>9</sup> and assuming that the transmission coefficient equals 1, as expressed in the following relation:

$$k(T) = (KT/h) \exp(-\Delta G^\ddagger/RT)$$

where  $\Delta G^\ddagger$  is difference between the Gibbs free energy of the reactant and the TS and  $K$  and  $h$  are the Boltzmann and Plank constants, respectively.

$\Delta G^\ddagger$  was calculated using the following relations:

$$\Delta G^\ddagger = \Delta H^\ddagger - T\Delta S^\ddagger$$

and,

$$\Delta H^\ddagger = V^\ddagger + \Delta ZVPE + \Delta E(T)$$

where  $V^\ddagger$  is the potential energy barrier and  $\Delta ZVPE$  and  $\Delta E(T)$  are the differences between the ZPVE values and the temperature corrections of the TS and the reactant, respectively.

## RESULTS AND DISCUSSION

### Kinetic and thermodynamic parameters

The gas-phase thermal decomposition of *N*-substituted *t*-butyl carbamates yields isobutylene and the corresponding carbamic acid in a slow step. The carbamic acids are unstable under the reaction conditions and decarboxylate rapidly to give carbon dioxide and the corresponding amine.

The kinetics of the rate-determining step in the decomposition of *N*-substituted *t*-butyl carbamates as well as the decarboxylation of the corresponding carbamic acids was examined. Geometries for the reactants, TS and products for the reactions under study were optimized using the Møller–Plesset perturbation method MP2 with a 6-31G basis set. Frequency calculations were carried under the average experimental conditions for this series of carbamates ( $T = 230^\circ\text{C}$ ). Thermodynamic quantities such as the ZPVE,  $E(T)$ , energy, enthalpy, and free energies were obtained from vibrational analysis. Entropy values were calculated from the vibrational analysis and using the factor  $C^{\text{exp}}$  suggested by Chuchani–Cordova.<sup>10</sup>

The results of the MP2 calculations for the rate-controlling step are shown in Table 1. A reasonable agreement was found for the calculated thermodynamic parameters  $\Delta H^\ddagger$ ,  $\Delta G^\ddagger$ ,  $\Delta S^\ddagger$  when compared to the experimental values. Calculated activation energies and rate coefficients are also in agreement with the experimental values.<sup>5</sup> Small but significant deviations of  $\Delta H^\ddagger$  and  $E_a$  values were found for the substrates with the substituents tetrahydropyrrole and 2-oxo-tetrahydropyrrole (Table 1). These differences may be due to mechanical errors during the experimental kinetics determinations for these substrates. Rate coefficients for the rate-determining step in the decomposition of *N*-substituted *t*-butyl carbamates from MP2/6-31G calculations show the same reactivity trend as the experimental values. The stronger the electron-withdrawing effect of the substituent on the nitrogen,

**Table 1.** Kinetic and thermodynamic parameters for the gas-phase elimination of *tert*-butyl carbamates Z-COO-C(CH<sub>3</sub>)<sub>3</sub>; Z = N(CH<sub>2</sub>CH<sub>3</sub>)<sub>2</sub>, NC<sub>4</sub>H<sub>8</sub>, NC<sub>4</sub>H<sub>6</sub>O, and NC<sub>4</sub>H<sub>4</sub> calculated at MP2/6-31G level at 230 °C. Experimental values are shown in parentheses

Z	$\Delta H^\ddagger$ (kJ mol <sup>-1</sup> )	E <sub>a</sub> (kJ mol <sup>-1</sup> )	$\Delta G^\ddagger$ (kJ mol <sup>-1</sup> )	$\Delta S^\ddagger$ (J mol <sup>-1</sup> K <sup>-1</sup> )	Log A	$k \times 10^4$ (sec <sup>-1</sup> )
-N(CH <sub>2</sub> CH <sub>3</sub> ) <sub>2</sub>	153.2 (154.4)	157.4 (158.6)	179.5 (180.7)	-52.2 (-52.3)	12.86 (12.87)	0.024 (0.018)
-NC <sub>4</sub> H <sub>8</sub>	155.9 (141.2)	160.1 (145.4)	176.1 (161.4)	-40.1 (-40.2)	11.4 (11.36)	0.055 (1.83)
-NC <sub>4</sub> H <sub>6</sub> O	152.6 (136.6)	156.8 (140.8)	171.1 (155.1)	-36.7 (-36.8)	11.5 (11.54)	0.18 (8.31)
-NC <sub>4</sub> H <sub>4</sub>	146.7 (141.0)	150.9 (145.2)	159.5 (153.8)	-25.4 (-25.5)	12.1 (12.12)	2.89 (11.03)

**Table 2.** Activation energies for the thermal decomposition of carbamic acids at 230 °C calculated at MP2/6-31G level of theory. No experimental data is available for this reaction due to the instability of the substrates under the reaction conditions

Z	E <sub>a</sub> (kJ mol <sup>-1</sup> )
-N(CH <sub>2</sub> CH <sub>3</sub> ) <sub>2</sub>	24.3
-NC <sub>4</sub> H <sub>8</sub>	26.1
-NC <sub>4</sub> H <sub>6</sub> O	28.9
-NC <sub>4</sub> H <sub>4</sub>	20.2

the greater the rate coefficient. The reaction for the pyrrole substituent is the fastest, followed by that of 2-oxo-tetrahydropyrrole, THP, and diethylamine: NC<sub>4</sub>H<sub>4</sub> > NC<sub>4</sub>H<sub>6</sub>O > NC<sub>4</sub>H<sub>8</sub> > N(CH<sub>2</sub>CH<sub>3</sub>)<sub>2</sub>. This suggests the stabilization of a negative charge developing on the ester-oxygen in the TS.

Parameters for decarboxylation of the intermediate *N*-substituted carbamic acids were also calculated at the MP2/6-31G level of theory. Experimentally, this was not possible due to the instability of the acids under the

reaction conditions. Calculated activation energies and rate coefficients for this step are shown in Table 2. Results for this step show that decarboxylation of the carbamic acids is significantly faster than in the previous step with activation energies for this step being in the order of 20–29 kJ/mol.

### Transition state and mechanism

Calculated values for the activation entropies for the rate-determining step vary from -25 to -52 J/mol K, which is consistent with a concerted process and a cyclic TS geometry. The TS for the gas-phase thermal decomposition of *N*-substituted *t*-butyl carbamates is a cyclic six-membered structure, in agreement with log A values between 11.5 and 12.8.<sup>11</sup>

Geometrical parameters for reactants and TSs are shown in Table 3. Distances and angles between the atoms involved in the reaction (O1, C2, O3, C4, C5, and H6) for all carbamates show that the TS geometry is a six-membered ring with the hydrogen being transferred (H6) midway between the carbon C5 and the oxygen O1

**Table 3.** Structural parameters for reactants and TS for *tert*-butyl carbamates Z-COO-C(CH<sub>3</sub>)<sub>3</sub>; Z = N(CH<sub>2</sub>CH<sub>3</sub>)<sub>2</sub>, NC<sub>4</sub>H<sub>8</sub>, NC<sub>4</sub>H<sub>6</sub>O, and NC<sub>4</sub>H<sub>4</sub>, from MP2/6-31G calculations at 230 °C. Atom distances are in Å and dihedral angles are in degrees

R	-N(CH <sub>2</sub> CH <sub>3</sub> ) <sub>2</sub>		-NC <sub>4</sub> H <sub>8</sub>		-NC <sub>4</sub> H <sub>6</sub> O		-NC <sub>4</sub> H <sub>4</sub>	
	R	TS	R	TS	R	TS	R	TS
	distances (Å)							
O1-C2	1.264	1.330	1.263	1.332	1.240	1.309	1.250	1.313
C2-O3	1.400	1.310	1.400	1.310	1.390	1.309	1.380	1.290
O3-C4	1.510	2.130	1.510	2.120	1.520	2.210	1.520	2.250
C4-C5	1.530	1.420	1.530	1.420	1.530	1.410	1.530	1.400
C5-H6	1.090	1.310	1.090	1.310	1.090	1.280	1.090	1.270
H6-O1	2.410	1.330	2.410	1.320	2.450	1.380	2.440	1.390
	Dihedral angles							
	TS		TS		TS		TS	
O1-C2-O3-C4	-23.861		24.860		29.323		24.197	
C2-O3-C4-C5	10.150		-11.330		-12.340		-10.530	
O3-C4-C5-H6	2.670		-2.060		-3.060		-2.330	
C4-C5-H6-O1	-16.640		17.510		21.630		20.020	
	TS imaginary frequency (cm <sup>-1</sup> )							
	-N(CH <sub>2</sub> CH <sub>3</sub> ) <sub>2</sub>		-NC <sub>4</sub> H <sub>8</sub>		-NC <sub>4</sub> H <sub>6</sub> O		-NC <sub>4</sub> H <sub>4</sub>	
	1482.2 i		1512.5 i		1311.8 i		1216.7 i	

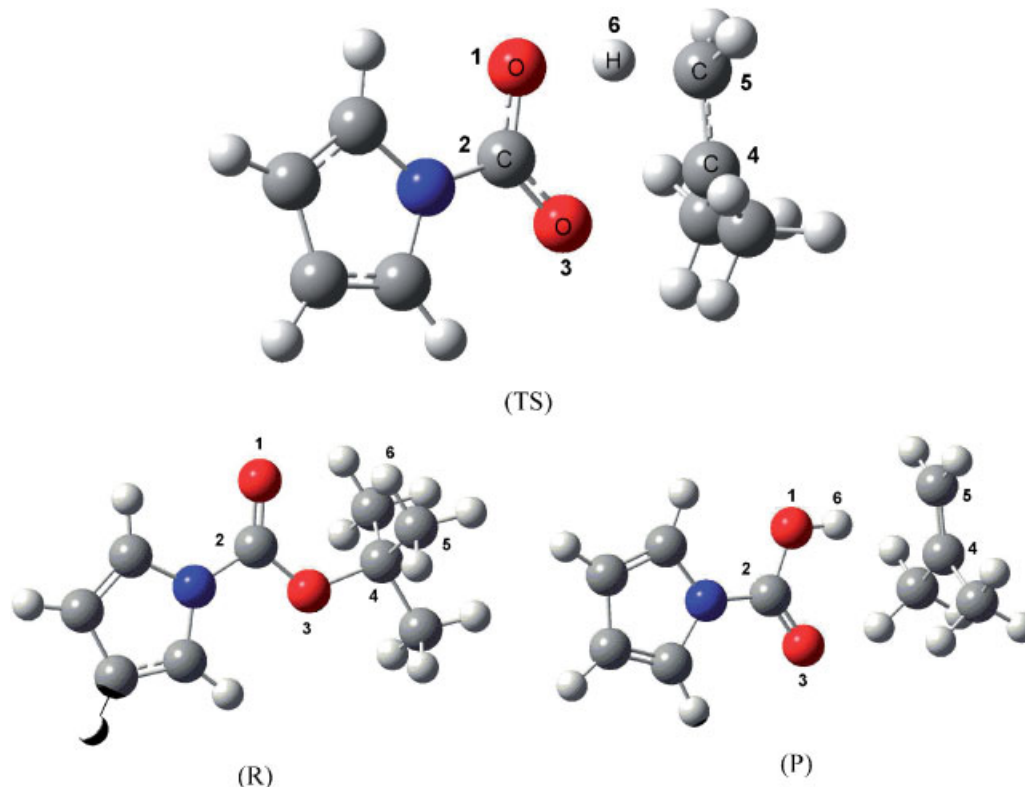
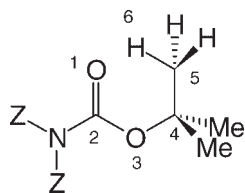


**Figure 1.** Optimized structures for reactant (*R*), transition state (TS) and intermediate products (*P*) for the rate determining step are shown for  $Z = \text{NC}_4\text{H}_4$ . TS geometries are a six-membered ring for all carbamates in this series

(Fig. 1, Scheme 2). TS structures show some departure from planarity as revealed by the reported dihedral angles, with a maximum deviation of  $23.7\text{--}29.3^\circ$ .

Comparison of the TS structure for the carbamates of this series showed similar geometries in terms of bond distances, except for the H6—O1 bond which is more elongated in the TS for substrates  $Z = \text{NC}_4\text{H}_6\text{O}$ , and  $-\text{NC}_4\text{H}_4$ . In other words, for substituents 2-oxo-THP and pyrrole the TS structure occurs early in this reaction coordinate (H6 hydrogen transfer from C5 to O1). Also the O3—C4 distance is slightly greater for 2-oxo-THP and pyrrole carbamate derivatives in the TS compared to the other substrates, implying that there is more progress in this reaction coordinate (late TS considering O3—C4 bond breaking).

The process is concerted in the sense that the C3—O4 and C5—H6 bond distances increase, showing breaking of these bonds ( $1.51\text{--}1.52$  to  $2.13\text{--}2.25$  Å in TS and  $1.09$  to  $1.31\text{--}1.28$  Å in TS, respectively). The C4—C5 and C2—O3 bond distances reveal a change from a single to



**Scheme 2**

double bond character ( $1.53$  to  $1.40\text{--}1.42$  Å in TS and  $1.40\text{--}1.38$  to  $1.31\text{--}1.29$  Å in TS, respectively) as the hybridization changes from  $sp^3$  to  $sp^2$ . The TV shows that the process is dominated by the elongation of the C3—O4 bond.

TSs for the rate determining step were characterized by unique imaginary frequencies:  $-1482.2$ ,  $-1512.5$ ,  $-1311.8$ , and  $-1216.7$   $\text{cm}^{-1}$  for  $Z = -\text{N}(\text{CH}_2\text{CH}_3)_2$ ,  $-\text{NC}_4\text{H}_8$ ,  $-\text{NC}_4\text{H}_6\text{O}$ , and  $-\text{NC}_4\text{H}_4$ , respectively, and these are associated with the displacement of hydrogen H6 from C5 to the carbonyl oxygen O1.

Natural bond orbital (NBO) charge analysis showed that the O3—C4 bond is highly polarized both in the reactant and TS structures, in the direction  $\text{O}3^{\delta-}\text{—C}4^{\delta+}$  (Table 4). Going from reactant to TS, the following changes in partial charge occur: an increase in the positive charge  $\delta+$  of the hydrogen H6 (from  $0.23$  to  $0.46$ ,  $0.48$  in TS), an increase in the negative charge of the carbonyl oxygen O1 ( $-0.72$ ,  $-0.78$  to  $-0.86$ ,  $0.83$  in TS) and an increase in the negative charge of O3 ( $-0.70$ ,  $-0.68$  to  $-0.85$ ,  $-0.83$  in TS). There is also an increase in the polarization at the O3—C4 bond (charge separation  $1.02\text{--}1.28$ ,  $1.30$  in TS). The bond polarization for the O3—C4 bond is  $0.268$  for *N*-substituted *t*-butyl carbamates  $Z = -\text{N}(\text{CH}_2\text{CH}_3)_2$ , and  $Z = \text{NC}_4\text{H}_8$ , and  $0.283$  and  $0.24$  for  $Z = \text{NC}_4\text{H}_6\text{O}$ , and  $-\text{NC}_4\text{H}_4$ , respectively. The latter two substituents decompose faster than the former two, following the reactivity order  $\text{NC}_4\text{H}_4 > \text{NC}_4\text{H}_6\text{O} > \text{NC}_4\text{H}_8 > \text{N}(\text{CH}_2\text{CH}_3)_2$ . An analysis of the NBO charges

**Table 4.** NBO charges for reactants and TS for *tert*-butyl carbamates Z-COO-C(CH<sub>3</sub>)<sub>3</sub>; Z = N(CH<sub>2</sub>CH<sub>3</sub>)<sub>2</sub>, NC<sub>4</sub>H<sub>8</sub>, NC<sub>4</sub>H<sub>6</sub>O, and NC<sub>4</sub>H<sub>4</sub> from MP2/6-31G calculations at 230 °C

Z	-N(CH <sub>2</sub> CH <sub>3</sub> ) <sub>2</sub>		-NC <sub>4</sub> H <sub>8</sub>		-NC <sub>4</sub> H <sub>6</sub> O		-NC <sub>4</sub> H <sub>4</sub>	
	R	TS	R	TS	R	TS	R	TS
O1	-0.778	-0.857	-0.775	-0.854	-0.692	-0.797	-0.723	-0.833
C2	1.100	1.107	1.106	1.113	1.109	1.117	1.125	1.130
O3	-0.696	-0.847	-0.694	-0.844	-0.695	-0.844	-0.684	-0.832
C4	0.326	0.440	0.325	0.436	0.326	0.460	0.327	0.473
C5	-0.712	-0.883	-0.712	-0.884	-0.713	-0.875	-0.714	-0.875
H6	0.273	0.472	0.272	0.473	0.273	0.463	0.270	0.462

together with the rate coefficients implies that O3—C4 bond polarization dominates the decomposition process, and that electron withdrawing groups stabilize the negative charge of the ester oxygen facilitating the decomposition process.

### Bond order analysis

NBO bond order calculations were performed.<sup>12–14</sup> Wiberg bond indexes<sup>15</sup> were computed using the NBO program<sup>16</sup> as implemented in Gaussian 98W, to further investigate the nature of the TS along the reaction pathway. The bond breaking and forming process involved in the reaction mechanism can be monitored by means of the Synchronicity (Sy) concept proposed by Moyano *et al.*<sup>17</sup> defined by the expression:

$$Sy = 1 - \frac{\left[ \sum_{i=1}^n |\delta B_i - \delta B_{av}| / \delta B_{av} \right]}{2n - 2}$$

where *n* is the number of bonds directly involved in the reaction. The relative variation of the bond index is obtained from:

**Table 5.** NBO analysis for thermal decomposition of *tert*-butyl carbamates Z-COO-C(CH<sub>3</sub>)<sub>3</sub>; Z = N(CH<sub>2</sub>CH<sub>3</sub>)<sub>2</sub>, NC<sub>4</sub>H<sub>8</sub>, NC<sub>4</sub>H<sub>6</sub>O, and NC<sub>4</sub>H<sub>4</sub> at 230 °C. Wiberg bond indexes (*B<sub>i</sub>*), % evolution through the reaction coordinate (%Ev), average bond index variation ( $\delta B_{av}$ ) and Synchronicity parameter (Sy) are shown

Z		O1—C2	C2—O3	O3—C4	C4—C5	C5—H6	H6—O1	$\delta B_{prom}$	Sy
-N(CH <sub>2</sub> CH <sub>3</sub> ) <sub>2</sub>	<i>B<sub>i</sub><sup>R</sup></i>	1.553	0.958	0.780	1.006	0.910	0.003	0.506	0.866
	<i>B<sub>i</sub><sup>TS</sup></i>	1.232	1.291	0.208	1.295	0.472	0.246		
	<i>B<sub>i</sub><sup>P</sup></i>	0.971	1.543	0.001	1.909	0.017	0.659		
	%Ev	55.2	57.0	73.4	32.0	49.0	37.0		
-NC <sub>4</sub> H <sub>8</sub>	<i>B<sub>i</sub><sup>R</sup></i>	1.557	0.955	0.784	1.006	0.910	0.003	0.507	0.871
	<i>B<sub>i</sub><sup>TS</sup></i>	1.231	1.290	0.214	1.296	0.467	0.251		
	<i>B<sub>i</sub><sup>P</sup></i>	0.970	1.547	0.001	1.910	0.016	0.663		
	%Ev	55.4	56.7	72.8	32.1	49.6	37.5		
-NC <sub>4</sub> H <sub>6</sub> O	<i>B<sub>i</sub><sup>R</sup></i>	1.667	0.972	0.769	1.007	0.910	0.003	0.502	0.842
	<i>B<sub>i</sub><sup>TS</sup></i>	1.332	1.338	0.162	1.295	0.504	0.218		
	<i>B<sub>i</sub><sup>P</sup></i>	1.034	1.597	0.001	1.908	0.020	0.651		
	%Ev	52.9	58.6	78.9	32.0	45.6	33.3		
-NC <sub>4</sub> H <sub>4</sub>	<i>B<sub>i</sub><sup>R</sup></i>	1.184	0.824	0.595	0.843	0.747	0.005	0.312	0.378
	<i>B<sub>i</sub><sup>TS</sup></i>	1.300	1.383	0.140	1.300	0.513	0.208		
	<i>B<sub>i</sub><sup>P</sup></i>	1.007	1.631	0.001	1.903	0.022	0.643		
	%Ev	65.7	69.3	76.5	42.7	32.3	31.8		

$$\delta B_i = \frac{[B_i^{TS} - B_i^R]}{[B_i^P - B_i^R]}$$

where the superscripts *R*, TS, and *P* represent the reactant, transition state, and product, respectively.

The bond change evolution is calculated as:

$$\%Ev = \delta B_i * 100$$

The average value is calculated from:  $\delta B_{ave} = \frac{1}{n} \sum \delta B_i$

Bonds indexes were calculated for the bonds involved in the reaction changes, that is: O1—C2, C2—O3, O3—C4, C4—C5, C5—H6, and H6—O1 (Scheme 2, Fig. 1); all other bonds remain practically unaltered during the process.

The calculated Wiberg indexes *B<sub>i</sub>* for the reactant, TS and products for *N*-substituted *t*-butyl carbamates (Z = —N(CH<sub>2</sub>CH<sub>3</sub>)<sub>2</sub>, —NC<sub>4</sub>H<sub>8</sub>, —NC<sub>4</sub>H<sub>6</sub>O, and —NC<sub>4</sub>H<sub>4</sub>), allow the progress of the reaction and the position of the TS between reactant and product (Table 5) to be examined. The Wiberg indexes show more progress in the O3—C4 bond breaking (73–79%) while the changes



in O1—C2, C2—O3, and C5—H6 bonds are intermediate in the reaction coordinate (52–55%), with the exception of the pyrrole derivative which shows a progress of 67% for O1—C2 and 69% for C2—O3 reaction coordinates. These results show that for the carbamate Z = pyrrole, there is more progress in the reaction for three reaction coordinates O3—C4 bond breaking, and O1—C2, C2—O3 bond order changes compared to the other carbamates. Moderate progress is observed for the C4—C5 double bond formation with 32–33% for carbamates Z = —N(CH<sub>2</sub>CH<sub>3</sub>)<sub>2</sub>, —NC<sub>4</sub>H<sub>8</sub>, —NC<sub>4</sub>H<sub>6</sub>O and 42% for the pyrrole derivative. The H6—O1 single bond formation is the reaction coordinate that shows less progress for all substrates (32–38%). In general, the reaction progress is more advanced for O3—C4 bond breaking; in addition, the O1—C2, C2—O3 bond order changes also show significant progress in the case of the pyrrole substituent.

Sy parameters reveal a concerted asynchronous process for all carbamates. There is relative progress for all reaction coordinates for carbamates Z = —N(CH<sub>2</sub>CH<sub>3</sub>)<sub>2</sub>, —NC<sub>4</sub>H<sub>8</sub>, —NC<sub>4</sub>H<sub>6</sub>O (Sy = 0.89), while for the pyrrole analog the process in the TS is more polar and asynchronous (Sy = 0.38). This is consistent with the TS structure, both in terms of distances, angles, and NBO charges as analyzed above. The TS structure shows more progress in the O3—C4 bond breaking compared to other reaction changes. This finding suggests that the polarization of this bond in the direction O3<sup>δ-</sup>—C4<sup>δ+</sup> is a determining factor in the gas-phase elimination of *N*-substituted *t*-butyl carbamates.

## CONCLUSIONS

The results of this study provide some additional evidence for the reported concerted type of mechanism.<sup>18</sup> Theoretical calculations suggest that the reaction proceeds through a concerted asynchronous mechanism. The TS structure of the rate-determining step for the gas-phase elimination of *N*-substituted *t*-butyl carbamates is a six-membered ring geometry with some departure from planarity. The transferred hydrogen is located halfway between carbonyl oxygen O1 and C5. Activation parameters are in reasonable agreement with experimental values for the MP2/6-31G level of theory for carbamates (Z = —N(CH<sub>2</sub>CH<sub>3</sub>)<sub>2</sub>, —NC<sub>4</sub>H<sub>8</sub>, —NC<sub>4</sub>H<sub>6</sub>O, and —NC<sub>4</sub>H<sub>4</sub>). The rate coefficients are of the same order

of magnitude following the sequence observed for the experimental values: pyrrole > 2-oxo-tetrahydropyrrole > THP > diethylamine. NBO charge analysis suggests that the polarization of the alkyl oxygen–carbon bond, in the direction O3<sup>δ-</sup>—C4<sup>δ+</sup>, is the determining factor in the decomposition process and that stabilization of the ester oxygen negative charge by electron withdrawing groups increases the reaction rate.

## REFERENCES

1. Herize A, Domínguez RM, Rotinov A, Nuñez O, Chuchani G. *J. Phys. Org. Chem.* 1999; **12**: 201–206.
2. Daly NJ, Ziolkowsky F. *J. Chem. Soc. Chem. Comm.* 1972; 911–912.
3. Luiggi M, Dominguez RM, Rotinov A, Herize A, Cordova M, Chuchani G. *Int. J. Chem. Kinet.* 2002; **34**: 1–5.
4. Ruiz Gonzalez JM, Loroño M, Cordova T, Chuchani G. *J. Mol. Structure (THEOCHEM)*. 2005; **732**: 55–61.
5. Brusco Y, Domínguez RM, Rotinov A, Herize A, Cordova M, Chuchani G. *J. Phys. Org. Chem.* 2002; **15**: 796–800.
6. Frisch MJ, Trucks GW, Schlegel HB, Scuseria GE, Robb MA, Cheeseman JR, Zakrzewski VG, Montgomery JA Jr, Stratmann RE, Burant JC, Dapprich S, Millam JM, Daniels AD, Kudin KN, Strain MC, Farkas O, Tomasi J, Barone V, Cossi M, Cammi R, Mennucci B, Pomelli C, Adamo C, Clifford S, Ochterski J, Petersson GA, Ayala PY, Cui Q, Morokuma K, Malick DK, Rabuck AD, Raghavachari K, Foresman JB, Cioslowski J, Ortiz JV, Stefanov BB, Liu G, Liashenko A, Piskorz P, Komaromi I, Gomperts R, Martin RL, Fox DJ, Keith T, Al-Laham MA, Peng CY, Nanayakkara A, Gonzalez C, Challacombe M, Gill PMW, Johnson B, Chen W, Wong MW, Andres JL, Head-Gordon M, Replogle ES, Pople JA. *Gaussian 98, Revision A.3*, Gaussian, Inc: Pittsburgh, PA, 1998.
7. McQuarrie D. *Statistical Mechanics*, Harper & Row: New York, 1986.
8. Foresman JB, Frish AE. *Exploring Chemistry with Electronic Methods* (2nd edn). Gaussian, Inc: Pittsburg, PA, 1996.
9. Benson SW. *The Foundations of Chemical Kinetics*. Mc-Graw-Hill: New York, 1960.
10. Rotinov A, Dominguez RM, Córdova T, Chuchani G. *J. Phys. Org. Chem.* 2005; **18**: 616–624.
11. (a) Benson SW, O'Neal HE. *J. Phys. Chem.* 1967; **71**: 2903–2921; (b) Benson SB. *Thermochemical Kinetics*. John Wiley & Sons: New York, 1968.
12. Lendvay G. *J. Phys. Chem.* 1989; **93**: 4422–4429.
13. Reed AE, Weinstock RB, Weinhold F. *J. Chem. Phys.* 1985; **83**(2): 735–746.
14. Reed AE, Curtiss LA, Weinhold F. *Chem. Rev.* 1988; **88**: 899–926.
15. Wiberg KB. *Tetrahedron* 1968; **24**: 1083–1095.
16. Gaussian NBO version 3.1.
17. Moyano A, Periclas MA, Valenti E. *J. Org. Chem.* 1989; **54**: 573–582.
18. Chuchani G, Nuñez O, Marciano N, Napolitano S, Rodríguez H, Domínguez M, Ascanio J, Rotinov A, Domínguez RM, Herize A. *J. Phys. Org. Chem.* 2001; **14**: 146–158.